# Functional connectivity fingerprints of the human pulvinar: decoding its role in cognition

Guedj, Carole; Vuilleumier, Patrik

**How to cite**

GUEDJ, Carole, VUILLEUMIER, Patrik. Functional connectivity fingerprints of the human pulvinar: decoding its role in cognition. In: NeuroImage, 2020, vol. 221, p. 117162. doi: 10.1016/j.neuroimage.2020.117162

This publication URL: https://archive-ouverte.unige.ch/unige:139157
Publication DOI: 10.1016/j.neuroimage.2020.117162

NeuroImage 221 (2020) 117162

Contents lists available at ScienceDirect

NeuroImage

journal homepage: www.elsevier.com/locate/neuroimage

# Functional connectivity fingerprints of the human pulvinar: Decoding its role in cognition

Carole Guedj *, Patrik Vuilleumier

*Neuroscience Department, Laboratory for Behavioral Neurology and Imaging of Cognition, University Medical School of Geneva, Campus BIOTECH H8, 9 Chemin des Mines, 1202, Geneva, Switzerland*

ARTICLE INFO

*Keywords:*
Pulvinar
Thalamo-cortical circuit
Connectivity
Parcellation
Meta-analysis

ABSTRACT

The pulvinar is the largest thalamic nucleus in the brain and considered as a key structure in sensory processing and attention. Although its anatomy is well known, in particular thanks to studies in non-human primates, its role in perception and cognition remains poorly understood. Here, we used resting-state functional connectivity from a large sample of high-resolution data provided by the Human Connectome Project, combined with a large-scale meta-analysis approach to segregate and characterize the functional organization of the pulvinar nucleus. We identified five clusters per pulvinar with distinct connectivity profiles and determined their respective co-activation patterns. Using the Neurosynth database, we then investigated the functional significance of these co-activation networks. Our results confirm the functional heterogeneity of the pulvinar, revealing clearcut differences across clusters in terms of their connectivity patterns and associated cognitive domains. While the anterior and lateral clusters appear to be involved in action and attention domains, the ventromedial and dorsomedial clusters may preferentially subserve emotional processes and saliency detection. In contrast, the inferior cluster shows less specificity but correlates with perception and memory processes. Collectively, our results suggest that the pulvinar underwrites different components of cognition, supporting a central role in the coordination of cortico-subcortical processes mediated by distributed brain networks.

## 1. Introduction

The pulvinar has long been considered as a key structure for information processing and communication across brain areas (Kanai et al., 2015; Sherman, 2016; Hwang et al., 2017; Gattass et al., 2018), but its exact functional organization remains poorly understood, especially in humans. A recent revival interest in the literature has emphasized its role in human cognition, particularly in attention processes (Gattass et al., 2018; Stitt et al., 2018; Fiebelkorn et al., 2019; Fiebelkorn and Kastner, 2019a; Jaramillo et al., 2019). Anatomical evidence in nonhuman primate showing extensive connections between the cortex and the pulvinar (Benevento and Rezak, 1976; Adams et al., 2000; Shipp, 2001, 2003; Kaas and Lyon, 2007) makes it a central node in large-scale networks, capable of integrating activity across distributed cortical areas (Sherman and Guillery, 2002; Saalmann et al., 2012; Saalmann, 2014; Quax et al., 2017; Arcaro et al., 2018).

Like other subcortical nuclei, the pulvinar is internally and histologically heterogeneous. In both nonhuman primate and human species, it has generally been divided into anterior, inferior, lateral, and medial subregions (Olszewski, 1952; Morel et al., 1997). Some finer subdivisions characterized by cytoarchitectonic and chemoarchitectonic methods (Gutierrez et al., 1995, 2000; Romanski et al., 1997; Stepniewska and Kaas, 1997; Adams et al., 2000) have been described in monkeys. Histochemical techniques together with studies of anatomical projections in nonhuman primate thus significantly contributed to our understanding of how the pulvinar is divided into sub-regions. Accordingly, the medial part is mainly connected with multimodal sensory association areas as well as with prefrontal and cingulate cortices; the anterior part has dense connections with somatosensory areas; and both the lateral and inferior parts widely project to occipital and temporal areas of the dorsal and ventral visual streams (Kaas and Lyon, 2007).

In human, Arcaro et al. (2015) described a topographic organization within the ventrolateral pulvinar with two distinct visual field maps, while they reported a coarser representation of contralateral visual space in the ventromedial and dorsolateral portions (see also Cotton and Smith, 2007; Schneider, 2011; DeSimone et al., 2015). A retinotopic organization of the pulvinar has also been reported in monkeys (Gattass et al., 1978; Bender, 1981), suggesting similarities across the primates'

* Corresponding author.
*E-mail address:* carole.guedj@unige.ch (C. Guedj).

https://doi.org/10.1016/j.neuroimage.2020.117162
Received 6 March 2020; Received in revised form 10 June 2020; Accepted 8 July 2020
Available online 11 July 2020

phylogenetic tree. Recent tractography methods with DTI also allow investigating subcortical structures in humans through their connections, with other regions. For instance, as in the nonhuman primate, the human pulvinar projects widely to the visual cortex, but also to several higher-level areas such as the frontal eye field and parietal cortex (Leh et al., 2008; Arcaro et al., 2015). However, while pulvinar anatomy is relatively well outlined by histological work in animal models, its functional organization in human remains unresolved, presumably because of its small size, its subcortical location, and the limits of standard brain imaging approaches.

Functionally, different sub-regions within the pulvinar seem to be involved in distinct domains (Grieve et al., 2000; Barron et al., 2015; Bridge et al., 2016; Arcaro et al., 2018). Lesion studies in human have revealed that patients with damage to the medial pulvinar present with fear recognition deficits (Ward et al., 2007), while patients with more anterior lesions exhibit spatial attention deficits (Ward et al., 2002; Arend et al., 2008). Other findings suggest reduced filtering of distractor stimuli after pulvinar lesion, predominating for visually or emotionally salient information after damage to dorsomedial or dorsolateral portions, respectively (Lucas et al., 2019). In healthy people, neuroimaging work reported pulvinar activation across various perceptual, attentional, and emotional tasks (Bourgeois et al., 2020). A recent meta-analysis investigated the functional connectivity of the pulvinar through co-activation probabilities with the rest of the brain across many task-related fMRI studies (Barron et al., 2015) and identified five different sub-regions with distinct co-activation maps. However, this study could not provide a precise behavioral categorizations of these different sub-regions, as the putative functional role of each sub-region was defined through the corresponding task domain meta-analytic data used to segregate the pulvinar and therefore limited by the inherent circularity of this approach. Thus, despite extensive work on pulvinar anatomy and evidence for an implication in multiple domains, its functional organization and how this relates to particular cognitive domains remain unresolved.

Here we aimed at investigating not only whether functionally distinct subregions exist in the human pulvinar, but also better characterizing their respective relationships with different cognitive domains. To do so, we took a novel multi-step approach. We first parcellated the pulvinar at the voxel-by-voxel level based on its whole-brain functional connectivity patterns at rest, using a large sample of high-resolution data from the Human Connectome Project. Then, we characterized whole-brain networks associated with each of these pulvinar sub-regions, either in the context of resting-state functional connectivity or in terms of co-activation statistics during task-based studies. Finally, we used the NeuroSynth database to meta-analytically 'decode' the functional significance of these networks.

Our approach reveals five distinct functional clusters in the pulvinar with specific pulvino-cortical connectivity fingerprints. By determining co-activation patterns for each of these clusters, we dissect the functional heterogeneity of the pulvinar and uncover clearcut differences across its subregions in terms of their cognitive profile.

## 2. Methods

### 2.1. Data and preprocessing

Resting-state fMRI (rs-fMRI) data were obtained from the Human Connectome Project (https://www.humanconnectome.org, Van Essen et al., 2013), under the 100 unrelated subjects database, acquired on the 3T Connectome Skyra. The minimally preprocessed dataset included 100 healthy subjects (age: 22–35, 46 males) with a gradient-echo planar sequence lasting 14.33 min (TR = 720 ms; TE = 33.1 ms; flip angle, 52°; FOV = 280 × 180 mm; 2 mm isotropic, 1200 TRs per runs). A total of two imaging runs for each individual were analyzed (first session). The minimal pre-processing pipeline included corrections for spatial distortions caused by gradient nonlinearities, head motion, $B_0$ distortion and registration to the T1-weighted structural image (Glasser et al., 2013). Additional preprocessing was performed using the AFNI software (Cox, 1996) and consisted of the following steps. Time courses were despiked and the right-left and left–right encoded runs were concatenated. A linear regression was applied to remove nuisance variables (estimated demeaned motion parameter and their temporal derivatives, mean time courses of the cerebrospinal fluid and white matter signals with linear and higher order polynomial trends) (Power et al., 2012; Van Dijk et al., 2012). Finally, a spatial smoothing with a 4-mm FWHM Gaussian kernel was applied to the output of the regression, in order to reduce the surrounding noise (Op de Beeck, 2010).

### 2.2. Functional parcellation of the pulvinar

We used a data-driven approach to divide the left and right pulvinar into distinct subregions according to their shared connectivity profiles with the rest of the brain (see methodological procedure Fig. 1). First, we created a mask of the left and right pulvinar separately using an atlas from Krauth et al. (2010), a digital model representing the three-dimensional anatomy of the thalamus and subthalamic structures (Krauth et al., 2010). For each rs-fMRI dataset, the time-courses of voxels belonging to the pulvinar mask and those belonging to the grey-matter mask (but excluding a dilated pulvinar mask) were separately extracted. To reduce the computation time and research space, we downsampled the voxels size of the grey-matter to $4 \times 4 \times 4$ $mm^3$. Next, to determine the functional connectivity of pulvinar voxels, we created a 2D cross-correlation matrix between these two sets of time-courses and transformed the Pearson correlation scores to z-values using the Fisher's r-to-z transformation. Each row of this cross-correlation matrix reflected the connectivity profile of a given pulvinar voxel with all cortical voxels of the brain.

Parcellation of the pulvinar was then performed for each individual using a standard K-means clustering method (implemented in the MATLAB Statistics Toolbox, using the "correlation" option as the distance measure). K-means is an iterative, non-hierarchical clustering algorithm that segments a region into K non-overlapping clusters by minimizing the within-cluster variance of each voxel in this region from the (randomly initialized) centroids. Given that we did not have a strong a priori hypothesis about the possible number of functional subregions of the pulvinar other than the multiarchitectonic anatomical subdivision into four nuclei proposed by Morel et al. (1997), we computed parcellations from K = 3 to K = 8 clusters. For each K, the best solution was chosen from 100 repetitions with a new centroids initialization each time.

Finally, to estimate a representative clustering group solution from all the individual partitioning obtained for each K, we adopted a consensus clustering approach (Monti et al., 2003; Janssen et al., 2015; Jeub et al., 2018). We computed a co-assignment matrix $\boldsymbol{Q}$ for each participant based on the individual clustering solution, where $q_{ij} = 1$ if voxel $i$ and $j$ are assigned to the same cluster and $q_{ij} = 0$ if voxel $i$ and $j$ are assigned to a different cluster. Co-assignment matrices were then averaged across subjects and the resulting mean matrix was submitted to a recursive K-mean clustering algorithm to obtain a partitioning group solution.

### 2.3. Determining the optimal number of cluster

To determine the optimal solution of K clusters at the group level, we considered three metrics based on topological consistency and information theory criteria. Identification of the optimal number of cluster remains a thorny issue that has not yet been fully solved in the computational science literature (e.g. Jain et al., 1999; Handl et al., 2005). The absence of a 'perfect' mathematical metric or algorithm to address this problem has led to multiple methods to provide estimates for optimal clustering. Here, our procedure was guided by a combination of criteria at the level of both individual and group solutions.

First, as a topological criterion, for a solution with K clusters, we assessed the percentage of voxels that were not related to the dominant parent cluster compared with the K-1 solution, either at the individual or group level clustering solution. This metric derives from the hierarchy of

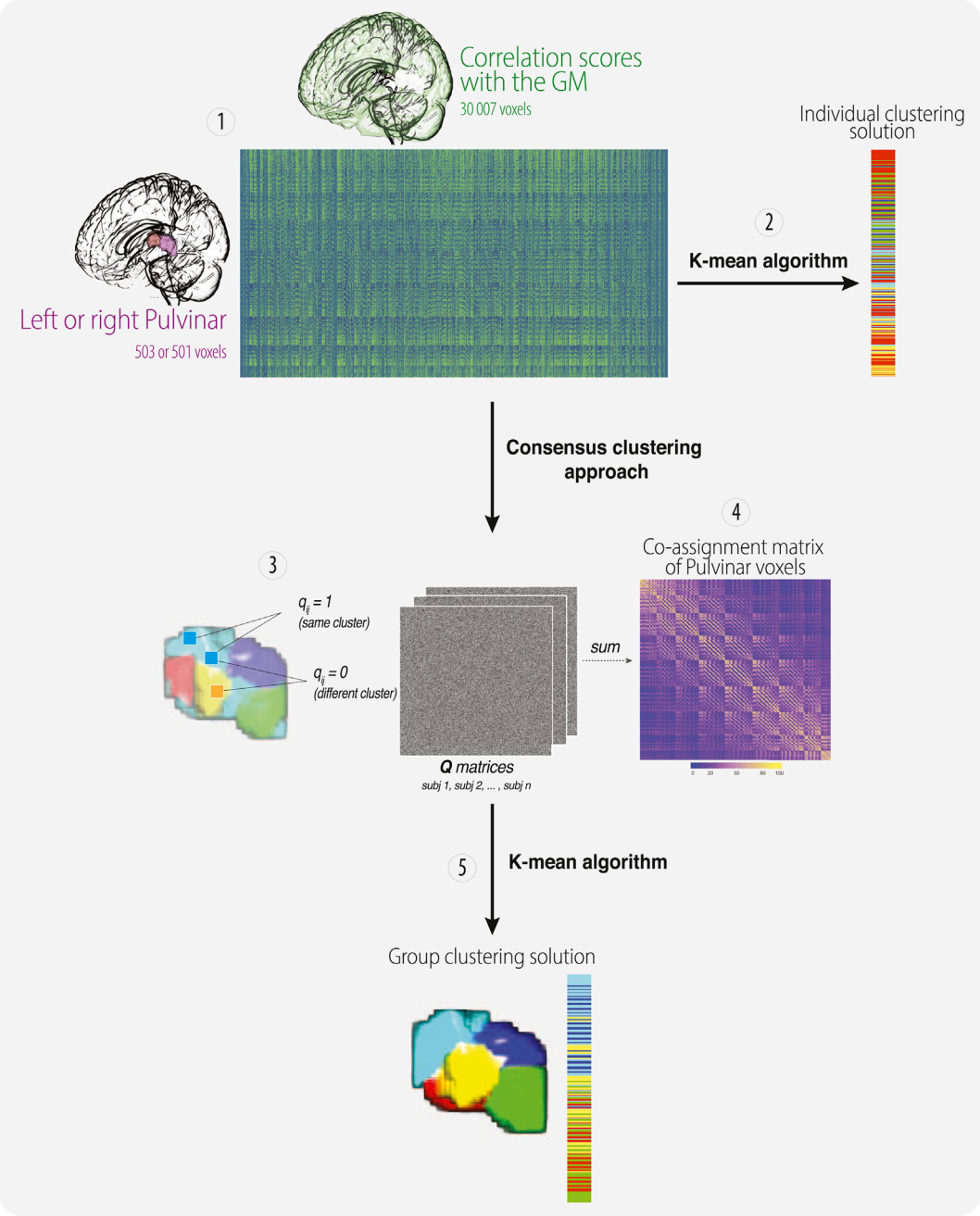


**Fig. 1. Method pipeline overview.** (1) Correlation matrix of rs-fMRI data for high-resolution left or right pulvinar voxels ($2 \times 2x2\ mm^3$) with concomitant data for low-resolution grey-matter (GM) voxels in the rest of brain ($4 \times 4x4\ mm^3$), excluding the pulvinar region. (2) Computation of the K-means algorithm (from K = 3 to K = 8) for each participant to obtain individual parcellation solutions. (3) Comparison of individual partitions to find a consensus partition at the group level, by computing co-assignment matrices for each participant. (4) Averaging of these matrices to obtain a co-assignment matrix over all subjects. (5) Computation of the K-mean algorithm on the average co-assignment matrix to obtain a final group clustering solution.

clusters (Kahnt et al., 2012) and corresponds to the number of voxels that are not consistent across the hierarchy, i.e., that disperse in a K solution to a cluster different from the parent cluster in the K-1 solution. We retained a 'good solution' for a given K parcellation when the percentage of lost voxels was below the median calculated across all other solutions.

Second, as a segregation criterion, we computed the silhouette value coefficient (Rousseeuw, 1987). This metric ranges from −1 to +1 and corresponds to the difference between the average distance of a voxel with the other voxels of its own cluster versus those in the other neighboring clusters. A 'good solution' was one with a higher silhouette score for K clusters (or at least no significant decrease of the silhouette coefficient) relative to the K-1 solution.

Finally, we calculated the variation of information (VI) index (Meilă, 2007) as a stability measure. The VI index is based on information theory and represents the shared information distance between clusters. Using a split-half comparison procedure, we randomly divided all participants into two equal groups. Then, we compared the clustering solution of one group (C) to the clustering solution of the other group (C') with the VI index. This procedure was repeated 100 times, each time with a different split-half group. Solutions with local minima of VI index, i.e., a significant decrease or increase of VI index compared to the previous or subsequent clustering solution, respectively, were considered stable.

### 2.4. Consistency of the best clustering solution

We assessed the spatial correspondence between clusters identified at the group-level and those identified in individual subjects. For each pair of group and individual cluster (*A,B*), we calculated the number of overlapping voxel using conjunction maps ($A \cap B$, where $\cap$ is the intersection between the two clusters). Then, we selected the cluster obtained at the individual-level with the highest degree of matching with each of the group clusters. Probability maps for each cluster were created by summing the binary conjunction maps across subjects. We also quantified the correspondence with traditional anatomical subdivisions of the pulvinar defined by Morel and colleagues (Morel et al., 1997; Krauth et al., 2010), using a percentage overlap for each cluster calculated as the number of shared voxels between a given cluster of the Morel's anatomical subdivision and a cluster of our functional subdivision, divided by the total number of voxels in the cluster of the Morel's anatomical subdivision.

### 2.5. Characterization of resting-state connectivity

In a next step, we characterized the brain networks associated with each of the pulvinar subregions identified by the clustering analysis described above. Importantly, to avoid a methodological bias related to circular analysis, this step was carried out on a different rs-fMRI dataset, which corresponded but using the second resting-state session of the original database. To ensure that the networks were statistically independent, we used a multilevel multiple regression approach. For each subject, we extracted the average time-course for each of the pulvinar subregions (left and right) identified at the group-level, and entered them into a multiple linear regression model. The resulting statistical t-maps were subject to Fisher's r-to-z transformation and thresholded at $Z > 4$ to retain only the most significant correlations. We then combined these maps at the group level using a two-way ANOVA, separately for each hemisphere, with the 'cluster' and 'participants' as fixed and random factors respectively. A false discovery-rate (FDR) adjusted p-value of $p < 0.001$ was used to create the statistical maps, which were then averaged across the two hemispheres.

### 2.6. Characterization of co-activation pattern

If the subdivisions revealed by the clustering analysis are meaningful, they should not only have a particular functional connectivity fingerprint at rest, but also reflect a distinctive activation pattern in task-based studies (Toro et al., 2008; Smith et al., 2009). To validate this prediction, we used the 'Neurosynth' database (http://neurosynth.org, Yarkoni et al., 2011), that contained activation data for 14′371 studies and reporting more than 150′000 brain locations at the time of our study (released July 2018). From this database, we identified the brain networks that co-activate with each symmetric (left and right taken together) pulvinar clusters using a meta-analytic approach (note that we also identified these networks for each cluster of each hemisphere separately, and given the strong overlap of co-activation patterns we have chosen to group them together). Activation in each voxel was represented as a binary vector of length corresponding to the total number of studies. A value of 1 indicated that at least 20% of the cluster of interest (in the pulvinar) was activated simultaneously with the given voxel (of the rest of the brain) and that it felt at the activation peak reported in a particular study, with a tolerance of 10 mm radius applied (i.e. a 0 value was attributed to the voxel if it was not within 10 mm of the reported focus) (Wager et al., 2009). For each voxel in the brain ($n = 231\,202$), statistical inference maps were then computed using a Chi-Square test of independence, with a significant result predicting the co-activation status (presence or absence of activation in each study). A false discovery-rate adjusted p-value of $p < 0.001$ was used to threshold the statistical maps.

Finally, to delineate regions commonly involved in task-dependent and task-independent functional connectivity of the each pulvinar cluster, we used a conjunction analysis using strict minimum statistics (Nichols et al., 2005), i.e. the voxels considered were those that were cumulatively statistically significant in the two analyses performed, using a common FDR-corrected threshold at $Z > 3$.

All connectivity maps (i.e. resting-state or co-activation, unthresholded maps), as well as the optimal parcellation of the pulvinar are available on Neurovault at https://identifiers.org/neurovault.collection:7959.

### 2.7. Meta-analytic decoding of network function

Another benefit of the Neurosynth database is the possibility to "decode" brain networks, based on automatically generated meta-analysis maps for thousands of behavioral or psychological terms. Thus, Neurosynth can be used to make quantitative inferences about the hypothetical cognitive functions associated with distributed activation patterns (Poldrack, 2011; Yarkoni et al., 2011). Here we calculated a voxel-wise Pearson correlation coefficient between the co-activation maps identified for each cluster and each of the 50 topic-based meta-analysis maps (Poldrack et al., 2012). Simply stated, a "topic" consists of an independent group of words that frequently occur together. The topics were generated by the Latent Dirichlet Allocation model (Blei et al., 2003) applied to the abstracts of all articles in the Neurosynth database in order to reduce semantic representation and avoid redundancy issue. This statistical model assumes that each article can be considered as a mixture of a small number of underlying 'topics', each of which are linked with a distribution over words. Thus, using Bayesian inference implemented by the MALLET toolbox we were able to estimate the topics and words distribution over the Neurosynth database (McCallum, 2002; Poldrack et al., 2012). For example, the 'pain' topic loads highly with the words 'painful', 'nociceptive', 'chronic', whereas the 'attention' topic loads highly with the words 'attentional', 'visual', 'target'. Topic maps were then created for each topic separately by comparing studies that loaded highly on a given topic with all other studies. Over the 50 generated topics, 23 were excluded because they concerned non-psychological phenomena such as methods or subject population (see Table S1 in Supplementary Material). Finally, we generated functional profiles by conducting correlation analyses between these topics maps and each of the pulvinar cluster's co-activation maps. These topics were then classified into four behavioral domains, namely *action*, *cognition*, *emotion,* and *perception*, in order to provide a more comprehensive characterization of pulvinar functions.

## 3. Results

### 3.1. Optimal parcellation of the pulvinar

We first parcellated the pulvinar at the voxel-by-voxel level based on data from the first resting-state session (2 runs) of 100 healthy individuals. Given a lack of any substantiated or apparent difference between the right and left pulvinar when examined separately (data not shown), our analysis considered the different topological and entropic criteria for clustering with the goal to identify a common solution for both hemispheres. At the individual level, the different metrics converged to the solutions $k = 5$ and $k = 6$. First, the percentage of voxels not related to the dominant parent was below the median for the solutions 6–7, 7–8 (left pulvinar), and 5–6, 6–7, 7–8 (right pulvinar) (see Fig. 2, top-left panel). Second, the segregation criterion was found to decrease with increasing divisions of the pulvinar, suggesting more effective partitioning with fewer clusters. However, the absence of significant differences for solutions ranging from 5 to 8 (left pulvinar) or from 6 to 8 (right pulvinar) indicated a good stability for these solutions (Fig. 2, top-middle panel). Third, the variation of information metric decreased (left pulvinar) or increased (right pulvinar) significantly from 3 to 4 clusters, but then increased significantly for both sides from 6 to 7 clusters with a local minima centered around the 5-cluster solution (Fig. 2, top-right panel).

At the group level, these metrics also converged to a 5-cluster solution

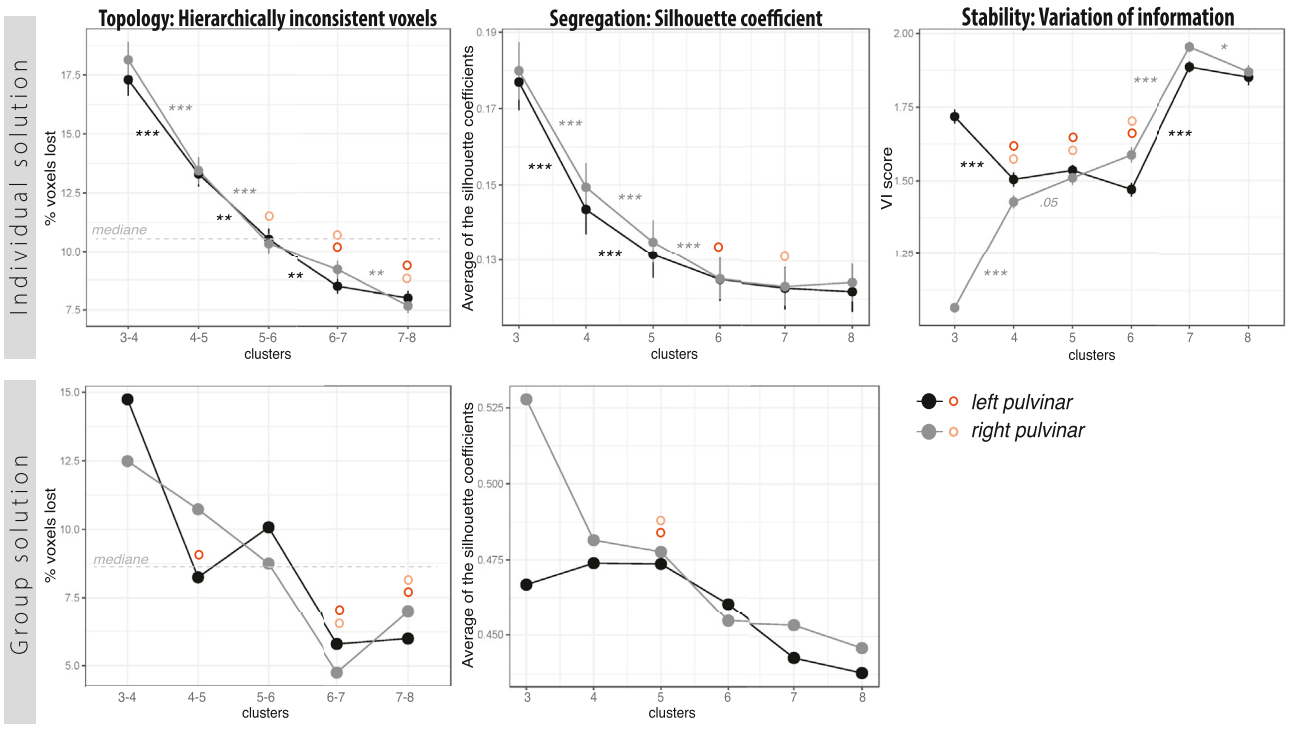


**Fig. 2. Metrics used to estimate the stability of cluster solutions.** [Left panel] Hierarchically inconsistent voxels, corresponding to the percentage of voxel not related to the dominant parent cluster compared with the K-1 solution, as a function of K, for the left (black dots) and right (grey dots) pulvinar, at the individual (top) and group (bottom) levels. The grey dotted line represents the median percentage. Small values indicate a low variation in topology. [Middle panel] Silhouette coefficients as a function of K, for the left (black dots) and right (grey dots) pulvinar, at the individual (top) and group (bottom) levels. High silhouette scores indicate an efficient segregation. [Right panel] VI index based on a split-half comparison procedure (100 repetitions) as a function of K, for the left (black dots) and right (grey dots) pulvinar, at individual level. A local minimum is an indicator of stability. The orange (left pulvinar) and light orange (right pulvinar) circles indicate the "good solutions" through the different panels. Collectively, these results point to an optimal solution with five clusters. Data are shown as means ± standard deviation; ***p value < 0.001; **p value < 0.01; *p value < 0.05.

(Fig. 2, bottom panel). First, the percentage of lost voxels was below the median for the 4–5, 6–7, 7–8 (left pulvinar) and for the 6–7, 7–8 solutions (right pulvinar) (Fig. 2, bottom-left panel). Second, a stability of the silhouette values was found for the 5-cluster solution (Fig. 2, bottom-right panel).

Therefore, based on these converging metrics, we selected a parcellation into 5 clusters as the optimal solution, showing good agreement between the different criteria and the two hemispheres, while avoiding an over-segmentation of the pulvinar.

This final group-level clustering solution is illustrated in Fig. 3A. It is remarkably symmetrical across the two hemispheres and splits the pulvinar into five regions: a dorsomedial cluster (cyan), a lateral cluster (blue), an anterior cluster (yellow), an inferior cluster (green), and a ventromedial cluster (red). Table 1 provides the coordinates of their centroid locations and respective sizes.

To estimate how well each cluster was consistent across subject, we calculated probability maps of matching with the group solution. As illustrated in Fig. 3B, we found an average overlay percentage of 57% (range 53%–62%) for the five-cluster solution. The most coherent across the participants was the anterior cluster, while the dorsomedial cluster was the least consistent (Fig. 3B, right panel). Overall, this shows a globally similar correspondence across individuals for all clusters.

We also quantified the degree of overlap of our partition with a classical anatomical subdivision of the pulvinar into four sub-regions based on atlas data (Morel et al., 1997; Krauth et al., 2010). As displayed in Fig. 3C, the anatomical inferior pulvinar subdivision overlapped perfectly with our inferior cluster, while the anatomical anterior pulvinar subdivision was mainly represented in our anterior cluster (and marginally in the dorsomedial cluster for the left side). In contrast, the anatomical lateral pulvinar subdivision was split into our inferior (primarily) and lateral (secondarily) clusters. Finally, the anatomical medial subdivision, which is the largest in this atlas, was dispersed across the other clusters with a small majority of voxels found in the dorsomedial cluster. It is noteworthy that the results were highly similar between our left and right partitions.

### 3.2. *Functional connectivity fingerprints of the pulvinar parcellation*

The primary concept behind parcellation based on functional connectivity is that voxels of the same functional unit in pulvinar should have a similar and specific resting-state signal correlated with the remaining voxels in the brain. Following this idea, we used another rs-fMRI dataset (second session of resting-state) to characterize the whole-brain functional connectivity patterns of each of the pulvinar clusters identified above. The obtained connectivity maps for each cluster are represented in Fig. 4 (first row).

Apart from the ventromedial cluster (red) that extended over the vast majority of the posterior neocortex, all other connectivity maps exhibited specific anatomical patterns. The dorsomedial cluster (cyan) was functionally connected with brain areas belonging to the default-mode network (DMN) and parts of the saliency network (SN), such as the medial and dorsolateral prefrontal cortex (DLPFC), anterior (ACC), posterior cingulate (PCC), inferior parietal lobule (IPL), and precuneus (Fox et al., 2005). The network associated with the lateral cluster (blue) extended to brain areas involved in executive control and attention such as the precentral (PreCG) and postcentral gyri (PostCG), middle frontal gyrus (MFG), superior (IPS) and inferior (IPL) posterior parietal cortex, superior temporal gyrus (STG), and precuneus, but also several regions in visual cortex such as fusiform gyrus (FG) and cuneus. The anterior cluster (yellow) was very selectively connected with areas belonging to

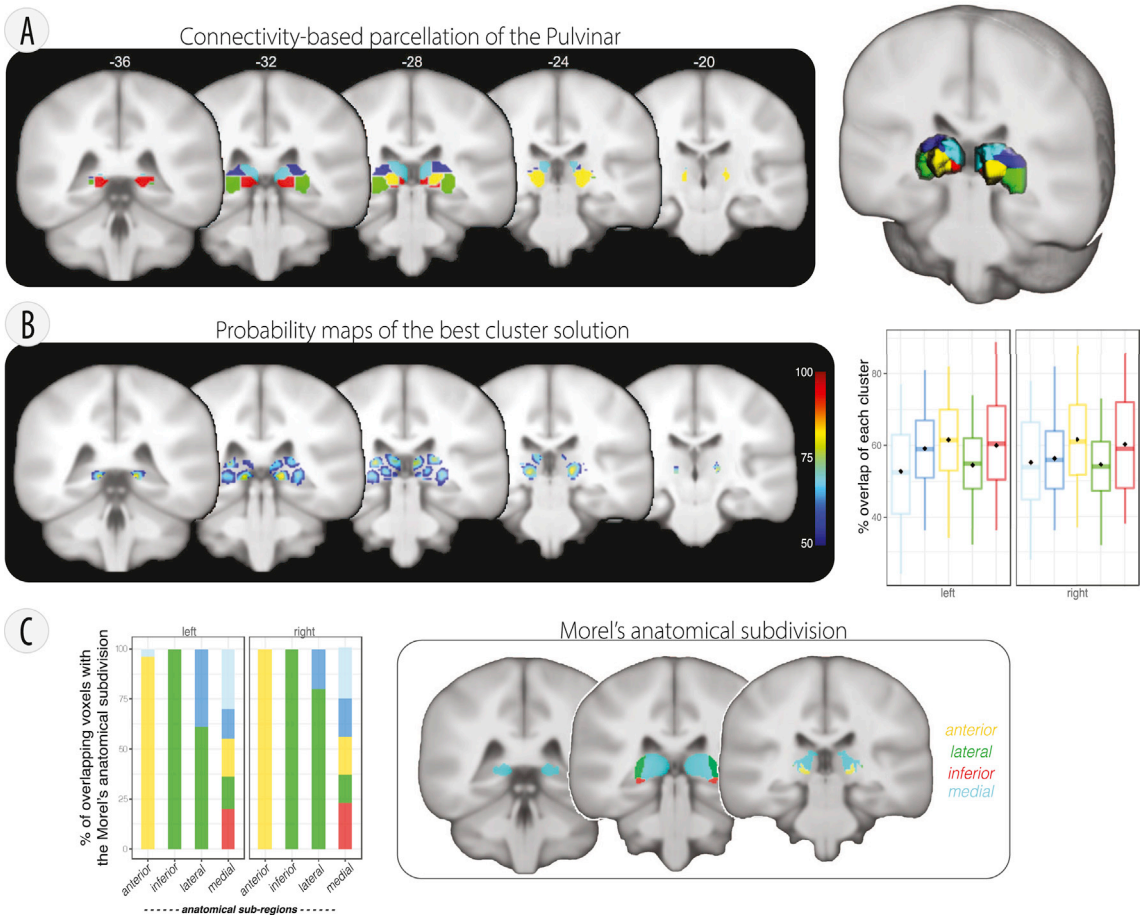


**Fig. 3. Connectivity-based parcellation of the human pulvinar.** (A) [Left panel] Final group-level clustering solution of the pulvinar split into five clusters: dorsomedial (cyan), lateral (blue), anterior (yellow), inferior (green), and ventromedial (red). The anatomical organization of the 5 clusters is highly similar in the two hemispheres. [Right panel] Three-dimensional surface rendering of the left and right pulvinar. (B) [Left panel] Probability maps of the five-cluster solution of the pulvinar, presented for each cluster separately (maps are thresholded at 50%). [Right panel] Distribution of overlapping scores of individual clusters relative to the group solution (percentage across participants) for each cluster. The black dots indicate the mean across voxels. (D) Percentage of overlapping voxels of our partition with the classical anatomical Morel's subdivision of the pulvinar into four sub-regions (see right-hand insert).

**Table 1**
Description of the optimal 5-cluster solution of the pulvinar clustering.

| Clusters | left | | | | right | | | |
|---|---|---|---|---|---|---|---|---|
| | X | y | z | cluster size | x | y | z | cluster size |
| dorsomedial (cyan) | −9 | −29 | 9 | 134 | 10 | −29 | 8 | 99 |
| lateral (blue) | −19 | −29 | 8 | 81 | 19 | −29 | 9 | 87 |
| anterior (yellow) | −13 | −25 | 3 | 94 | 15 | −25 | 4 | 100 |
| inferior (green) | −22 | −30 | 0 | 118 | 24 | −30 | 0 | 122 |
| Ventromedial (red) | −11 | −32 | 1 | 76 | 14 | −32 | 1 | 93 |

x, y, z coordinates refer to the centroid location in MNI space (LPI orientation). The cluster size refers to the number of voxels.

sensorimotor systems such as the PreCG, PostCG, and the medial frontal gyrus (MedFG) (Hutchison and Everling, 2012; Mueller et al., 2013). Finally, the inferior cluster (green) was also selectively coupled with early visual areas in occipital cortex (V1,V2, V3). Together, these data highlight a distinctive and widespread functional relationship of each pulvinar cluster with largescale brain networks.

### 3.3. Co-activation patterns of the pulvinar parcellation

To link brain networks connected to pulvinar clusters with particular functions, we further investigated the pattern of brain activation associated with task-induced modulation of each cluster, as reported in the Neurosynth database (Yarkoni et al., 2011; Poldrack et al., 2012). The resulting co-activation maps are illustrated in Fig. 4 (second row). In general, these co-activation networks were more widespread within subcortical areas than the task-independent networks identified by functional connectivity at rest above. The dorsomedial cluster (cyan) was primarily coupled with nodes of the salience network (SN) such as ACC, orbitofrontal cortex, striatum, and anterior insula (Seeley et al., 2007; Menon and Uddin, 2010). The lateral cluster (blue) co-activated with regions involved in attentional processing and executive functions, particularly the frontal-eye-field and superior parietal lobule (SPL)/intra-parietal sulcus (IPS), but also a few other areas in DLPFC, STG, and precuneus (Corbetta and Shulman, 2002; Corbetta et al., 2008). Very much like resting-state connectivity, the anterior cluster (yellow) showed strong coupling with motor and somatosensory areas including the PreCG and PostCG, supplementary motor area (SMA), as well as the basal ganglia, superior colliculus, and cerebellum. The inferior cluster (green) co-activated with several regions of visual cortex, mainly along the ventral extrastriate pathways such as the lingual gyrus, fusiform gyrus (FG), and middle occipital gyrus (MOG), but also with the amygdala and a few other regions associated with executive functions such as the

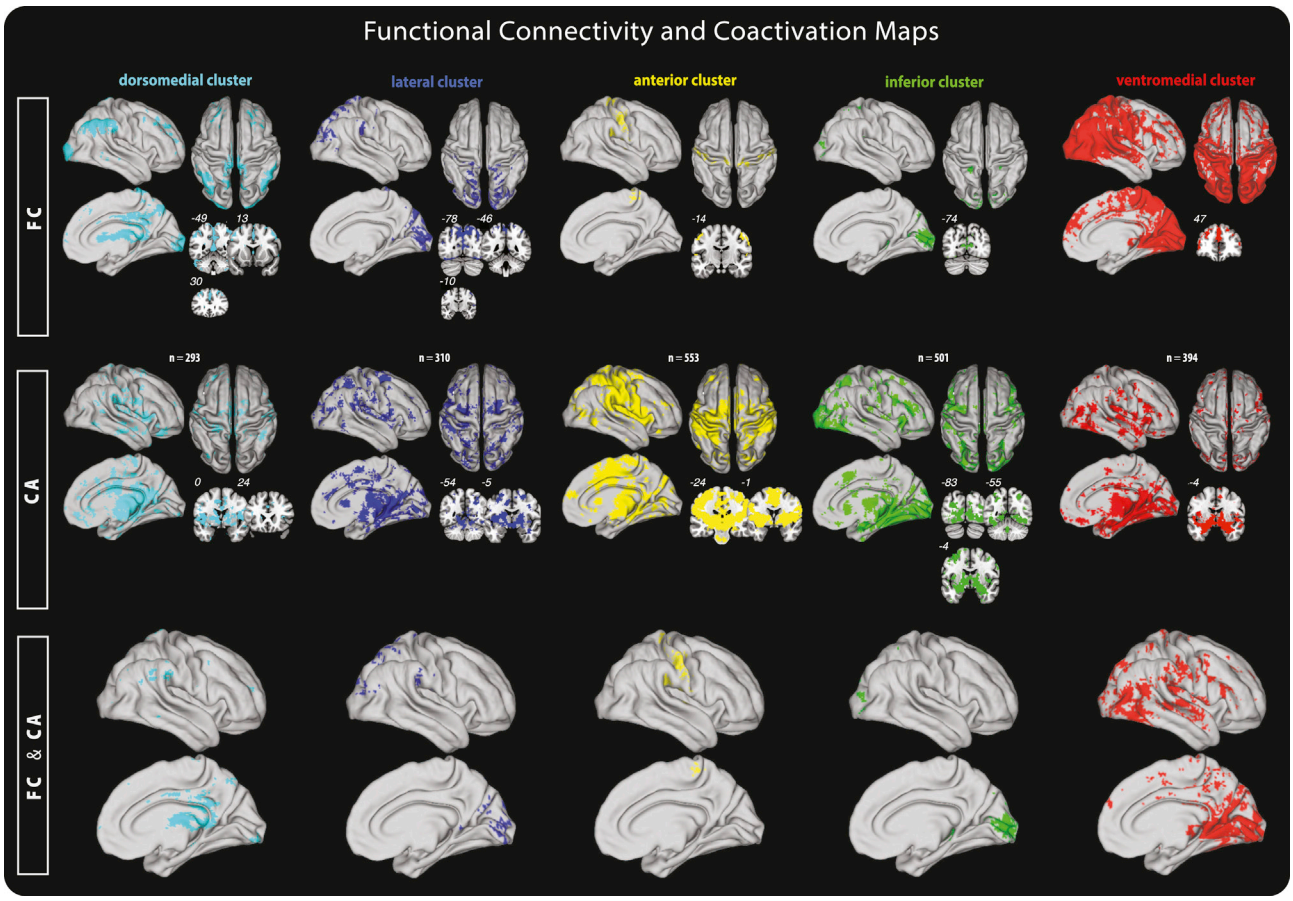


**Fig. 4. Functional connectivity and co-activation patterns of the pulvinar clusters.** [Top row] Resting-state functional connectivity profiles (FC) for each pulvinar cluster, based on correlation analysis of time-courses. [Middle row] Task-related co-activation patterns (CA) for each pulvinar cluster, based on meta-analytic analysis (Neurosynth). All maps are FDR-corrected at $p < 0.001$. [Bottom row] Conjunction of FC and CA results (thresholded at $Z > 3$). n = number of study selected to create the given co-activation map.

**Table 2**
Overlapping clusters between the functional connectivity and co-activation analyses.

| Regions | brodmann area | x | y | z | cluster size | regions | brodmann area | x | y | z | cluster size |
|---|---|---|---|---|---|---|---|---|---|---|---|
| dorsomedial cluster | | | | | | anterior cluster | | | | | |
| R IPL | area 40 | 60 | −30 | 30 | 115 | L PreCG | area 3 | −47 | −21 | 45 | 1462 |
| R Fusiform gyrus | area 37 | 54 | −59 | −23 | 201 | R PreCG | area 3 | 51 | −19 | 39 | 1470 |
| L Precuneus | area 19 | −36 | −75 | 41 | 121 | R MedFG | area 6 | 1 | −27 | 62 | 204 |
| R Lingual gyrus | area 18 | 13 | −89 | −15 | 206 | L Thalamus (Pulvinar) | | −13 | −23 | 3 | 242 |
| ACC | area 32 | 0 | 35 | 29 | 335 | R Thalamus (Pulvinar) | | 15 | −23 | 4 | 246 |
| | area 24 | 0 | −6 | 42 | 350 | **inferior cluster** | | | | | |
| Thalamus (Pulvinar) | | −1 | −31 | 14 | 3369 | L MOG | area 19 | −30 | −91 | 8 | 116 |
| **lateral cluster** | | | | | | L Cuneus | area 17 | 0 | −87 | 7 | 1392 |
| L PostCG | area 3 | −56 | −23 | 43 | 103 | L Thalamus (Pulvinar) | | −22 | −30 | −2 | 394 |
| R PostCG | area 2 | 50 | −29 | 52 | 115 | R Thalamus (Pulvinar) | | 24 | −29 | −1 | 429 |
| L IPL | area 40 | −43 | −40 | 56 | 127 | **ventromedial cluster** | | | | | |
| L ParaCL | area 5 | −2 | −44 | 55 | 110 | L IFG | area 46 | −45 | 38 | 14 | 186 |
| L SPL | area 7 | −26 | −60 | 58 | 187 | L PreCG | area 6 | −44 | −8 | 45 | 502 |
| R Fusiform gyrus | area 37 | 50 | −60 | −18 | 107 | R PreCG | area 4 | 19 | −32 | 68 | 121 |
| R Precuneus | area 7 | 20 | −70 | 54 | 300 | L STG | area 21 | −62 | −23 | −3 | 131 |
| R MTG | area 19 | 35 | −82 | 22 | 161 | L Precuneus | area 19 | −35 | −77 | 34 | 370 |
| L Cuneus | area 19 | −8 | −81 | 35 | 290 | PCC | area 29 | 6 | −47 | 9 | 21 954 |
| | | −28 | −87 | 23 | 191 | | | | | | |
| R Cuneus | area 17 | 6 | −86 | 2 | 357 | | | | | | |
| | area 19 | 16 | −93 | 22 | 133 | | | | | | |
| L Thalamus (Pulvinar) | | −20 | −30 | 9 | 258 | | | | | | |
| R Thalamus (Pulvinar) | | 19 | −29 | 10 | 293 | | | | | | |

x, y, z coordinates refer to the centroid location in MNI space (LPI orientation). The cluster size refers to the number of voxels.
Conjunction analysis between functional connectivity and co-activation maps ($Z > 3$, FDR corrected); extent threshold of 100 voxels. Abbreviations: L, left; R, right; ACC, anterior cingulate cortex; IFG, inferior frontal gyrus; IPL, inferior parietal lobule; MedFG, medial frontal gyrus; MTG, middle temporal gyrus; MOG, middle occipital gyrus; ParaCL, paracentral gyrus; PreCG, precentral gyrus; PostCG, postcentral gyrus; STG, superior temporal gyrus.

dorsolateral prefrontal cortex, posterior parietal cortex, and superior colliculus. Finally, the network associated with the ventromedial cluster (red) primarily encompassed the medial temporal lobe and subcortical areas such as the amygdala, hippocampus and parahippocampal area, plus ventral striatum and ventral visual extrastriate areas.

Furthermore, we determined statistically significant brain regions that were jointly identified by both the task-related co-activation and the resting-state connectivity patterns, using a conjunction analysis of these two results. Common areas are shown in Fig. 4, last row, and their coordinates are summarized in Table 2. The resulting conjunction maps confirm distinct network associated with each cluster.

### 3.4. Decoding of network function

Lastly, we used the Neurosynth database to meta-analytically decode the behavioral and psychological processes associated with the networks that co-activated with pulvinar clusters. We correlated each of the task-based co-activation networks (see previous section) with 23 selected topics maps from Neurosynth (see Table S1 in Supplementary Material), and then computed the average correlation scores for each behavioral domain. Please note that this approach is purely qualitative and does not provide any degree of significance for the calculated correlations.

Fig. 5A shows the pattern of behavioral domains for each co-activation network. Two of them exhibited strong specificity: the anterior cluster's network was highly associated with the action domain, while the ventromedial cluster's network was highly linked to the emotional domain. The dorsomedial and the lateral clusters' networks showed more general and relatively similar profiles, but with preferential links to emotion and action, respectively. In contrast, the inferior cluster's network was also generally involved with all domains, but preferentially with cognition.

Fig. 5B further presents correlation scores for the top ten topics that were the most frequently implicated across the whole set of co-activated networks (see Table 3 for more details about these topics). Topics related to cognition (green, 4 topics) and perception (blue, 3 topics) were found across all networks. A few more specific topic terms were related to particular networks only, in agreement with the general behavioral domains above (Fig. 5A). Thus, we found a strong specificity of the anterior cluster's network for motor processes (positive correlation, $r = 0.47$), and of the ventromedial cluster's network with emotional processes including pain ($r = 0.12$) and emotional faces ($r = 0.18$). The dorsomedial and the lateral clusters' networks shared associations with several cognitive processes, with slightly stronger implication of emotion/pain for the former and motor/task performance for the latter. Finally, the inferior cluster's network showed a preferential correlation with cognition and perception, particularly face recognition ($r = 0.21$) and memory ($r = 0.19$).

**Table 3**
Description of the ten most represented topics through the identified co-activation maps.

| Topics | *ID #* | *Num. studies* | Correlation coefficient (Pearson) | | | | | Domains |
|---|---|---|---|---|---|---|---|---|
| | | | dmPUL | latPUL | antPUL | infPUL | vmPUL | |
| Motor | *49* | *1076* | 0.11 | 0.16 | 0.47 | −0.06 | −0.1 | Action |
| motor, movement, movements, imagery, sensorimotor, primary, finger, areas, control, activation, sensory, tapping, force, somatosensory, tasks, execution, subjects, bimanual, mi, coordination, active, activated, imagined, timing, ipsilateral, voluntary, paced, cortices, simple, gait, healthy, network, pre, performed, system, planning, passive, walking, grip, sequential. | | | | | | | | |
| Memory | *12* | *1212* | −0.05 | 0.02 | −0.24 | 0.19 | 0.14 | Cognition |
| memory, retrieval, encoding, recognition, episodic, items, successful, recall, memories, words, information, subsequent, recollection, item, test, autobiographical, participants, context, event, associative, source, events, semantic, word, studied, pairs, encoded, familiarity, false, performance, term, judgments, associations, formation, correct, phase, success, remembered, support, suggest. | | | | | | | | |
| Task performance | *2* | *2680* | 0.08 | 0.11 | 0.2 | 0.09 | 0.03 | |
| task, performance, cognitive, tasks, control, activation, executive, behavioral, increased, difficulty, switching, function, network, accuracy, recruitment, performing, functions, performed, demands, ability, attention, correlated, set, participants, time, test, cognition, difficult, adults, level, goal, subjects, levels, visuospatial, switch, behavioural, monitoring, suggest, compared, perform. | | | | | | | | |
| Language | *7* | *389* | 0.07 | 0.09 | 0.19 | 0.03 | 0.02 | |
| language, hemispheric, lateralization, asymmetry, olfactory, lateralized, dominance, areas, odor, handed, laterality, dominant, handers, asymmetries, odors, specialization, drawing, handedness, functional, processing, interhemispheric, unilateral, leftward, sided, difference, patterns, cp, strongly, activations, test, indices, chemosensory, functions, spatial, measured, individual, investigated, asymmetric, index, humans. | | | | | | | | |
| Inhibition | *8* | *522* | 0.13 | 0.08 | 0.17 | −0.03 | 0.02 | |
| inhibition, response, inhibitory, control, stop, acupuncture, motor, signal, task, trials, nogo, error, suppression, responses, itch, activation, successful, phobia, inhibit, pre, trial, role, inhibiting, inhibited, phobic, spider, action, reactive, behavior, acupoint, stopping, sst, prepotent, monitoring, phobics, rifg, impulse, evoked, reduced, errors. | | | | | | | | |
| Emotional faces | *23* | *839* | 0.00 | −0.07 | −0.14 | 0.07 | 0.18 | Emotion |
| emotional, faces, facial, emotion, expressions, neutral, processing, fear, fearful, happy, social, threat, emotions, face, responses, response, disgust, angry, anxiety, sad, expression, perception, recognition, affective, affect, anger, threatening, signals, participants, sadness, anxious, individuals, cues, reactivity, masked, sensitivity, viewing, happiness, emotionally, alexithymia. | | | | | | | | |
| Pain | *48* | *585* | 0.27 | 0.14 | 0.37 | −0.05 | 0.12 | |
| pain, painful, stimulation, somatosensory, intensity, chronic, placebo, noxious, sensory, processing, induced, evoked, autonomic, responses, heat, nociceptive, primary, central, areas, cortices, secondary, perception, stimulus, analgesia, experience, ratings, sensation, system, thermal, modulation, skin, hyperalgesia, healthy, cold, perceived, interoceptive, patients, mechanisms, affective, treatment. | | | | | | | | |
| Object | *1* | *804* | −0.15 | −0.02 | −0.13 | 0.2 | 0.07 | Perception |
| object, category, visual, body, knowledge, categories, scenes, scene, representations, features, categorization, representation, images, perceptual, conceptual, participants, stimulus, abstract, selective, pictures, information, recognition, context, concepts, experience, bodies, categorical, natural, animals, space, similarity, level, human, represented, semantic, familiar, place, view, image. | | | | | | | | |
| Stimulation | *35* | *579* | 0.1 | 0.11 | 0.38 | −0.13 | −0.1 | |
| stimulation, somatosensory, tms, tactile, primary, rtms, touch, motor, areas, transcranial, body, tdcs, applied, induced, magnetic, sensory, human, representation, ipsilateral, repetitive, stimulated, secondary, muscle, swallowing, subjects, sensorimotor, site, healthy, finger, somatotopic, hz, perception, intensity, excitability, system, electrical, evoked, stimulus, leg, bladder. | | | | | | | | |
| Faces recognition | *5* | *566* | −0.12 | −0.05 | −0.21 | 0.21 | 0.15 | |
| face, recognition, processing, identity, familiar, unfamiliar, selective, response, perception, adaptation, voice, fg, familiarity, visual, person, responses, famous, facial, images, sensitive, compared, information, image, voices, effect, stimulus, laughter, people, human, names, participants, behavioral, repetition, selectivity, trustworthiness, normal, representation, viewed, viewing. | | | | | | | | |

Top terms associated with each topic. ID# = identity number related to the Neurosynth 'v4-topics-50' database. Num. studies = number of studies associated with each topic.

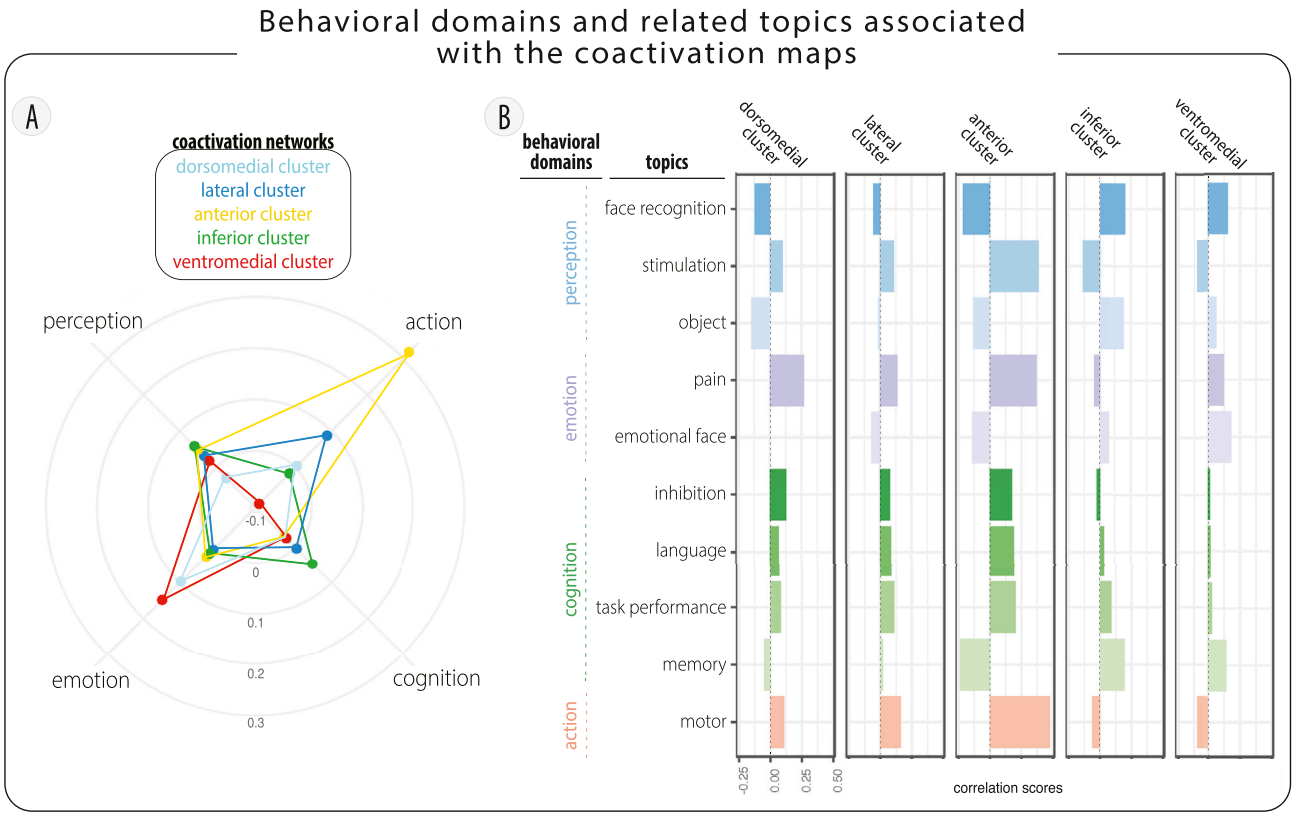


**Fig. 5. Functional decoding of the pulvinar clusters.** (A) Pattern of behavioral domains and related topics associated with each co-activation network, based on the Neurosynth database. The values reflect average Pearson correlation coefficients across topics that are associated with each domain. (B) Correlation scores of the top ten most represented topics (across all networks), plotted for each network separately.

## 4. Discussion

Understanding the role of the pulvinar in human cognition is a challenging question (Fiebelkorn and Kastner, 2019b). It has been implicated in various functions such as attention (e.g. (Petersen et al., 1987; Kastner et al., 2004; Shipp, 2004; Lucas et al., 2019), emotion and social recognition (Morris et al., 1999; Bertini et al., 2018), but also voluntary actions and saccades (Kaas and Lyon, 2007; Berman and Wurtz, 2011; Wilke et al., 2018), suggesting an important functional heterogeneity. Accordingly, neuroanatomical investigations point to the existence of several sub-nuclei within the pulvinar (Gutierrez et al., 1995; Stepniewska and Kaas, 1997). Here, we used a data-driven approach to dissect its functional connectivity with cortical networks in order to capture its intrinsic organization and putative roles.

### 4.1. Anatomical versus functional subdivisions

Based on resting-state connectivity with the rest of the brain, we found a robust subdivision into five units: dorsomedial, ventromedial, lateral, anterior, and inferior. Previous attempts to anatomically subdivide the pulvinar identified four main regions based on cyto- and chemoarchitectonic criteria (Olszewski, 1952; Morel et al., 1997). Compared to an influential atlas which described a very large medial sub-region relative to the others (Morel et al., 1997), our parcellation is more proportioned with a more or less similar size for each of the clusters. The smallest subdivisions in this atlas were the most consistent with our functional partition. Conversely, their medial subdivision was found to divide into different clusters in our partition, suggesting that the larger the anatomical subdivision, the more heterogeneous its functional profile.

### 4.2. Functional connectivity fingerprints reflect anatomical projections

Our results reveal distinct functional connectivity fingerprints associated with each pulvinar cluster. These functional maps presumably reflect the topology of anatomical projections from pulvinar to cortex, which follow a particular organization with a main rostrolateral to caudomedial gradient that is reflected in an occipital-frontal axis along the cortex (Shipp, 2001, 2003; Arcaro et al., 2015). Indeed, we found that networks coupled with the ventromedial and dorsomedial cluster were those extending most anteriorly in frontal cortices, while networks associated with the lateral and inferior clusters predominated over posterior cortical areas. Other studies described a dorso-ventral axis in pulvinar projections, similarly reflected at the cortical level (Baleydier and Morel, 1992; Baizer et al., 1993; Shipp, 2003). Accordingly, we also observed a dorso-ventral dissociation whereby the lateral cluster's network extended dorsally towards the parietal and superior temporal areas, unlike the inferior cluster's network extending more ventrally. Finally, although rarely studied in the literature, the anterior pulvinar was reported to project towards the somatosensory cortex (Jones, 2012), consistent with a tight coupling with sensorimotor areas observed here.

The ventromedial cluster exhibited a less clear connectivity profile than other clusters, with diffuse functional connectivity at rest but more restricted correlation with medial temporal lobe regions for task-based activations. Various elements could explain this pattern. First, the location of the ventromedial cluster was close to the pretectothalamic lamina, which contains a high density of myelinated fibers (Márquez-Legorreta et al., 2016). Although white matter signal was regressed out in our analysis using an erode mask (Jo et al., 2010), it could contribute to apparent global fluctuations of fMRI activity during resting state. Another possibility is the proximity of the ventromedial cluster to the choroidal artery (Neau and Bogousslavsky, 1996), which could also

generate global physiological noise reflecting cardiovascular rather than neural activity (Murphy et al., 2013). These aspects would not contaminate the task-based co-activation maps. Finally, a third possibility is that diffuse functional connectivity of the ventromedial cluster may reflect global influences of neuromodulators with widespread cortical projections, such as those implicated in arousal (Berridge and Waterhouse, 2003; Guedj et al., 2017) and possibly recruited during emotional-social conditions (see Fig. 5). In the same vein, the medial part of the pulvinar is mainly composed of matrix cells (i.e., calbindin-immunoreactive neurons) that project widely and diffusely over the cortex (Jones, 2001; Müller et al., 2020) and could thus account for more distributed patterns of functional coupling. Our results also converge with a recent parcellation of the thalamus using 3D gradient modelling of functional connectivity with fMRI (Tian et al., 2020), in which three posterior clusters (DP, VPl, and VPm) were found that partly overlapped with the pulvinar and mainly distinguished between our dorso-ventral and medio-lateral groups of nuclei.

Importantly, all functional connectivity maps observed in rs-fMRI data showed substantial shared territories with co-activation maps defined by the meta-analytical analysis of task-based studies. However, several dissimilarities were noticeable between the two patterns, in contrast with other studies highlighting strong overlaps between functional networks identified with these two approaches (e.g. Cauda et al., 2011). This observation might reflect the fact that the pulvinar's coupling with cortical networks could be more dependent on the context, leading to some variability between resting-state connectivity patterns and the task-based co-activation patterns, in keeping with the notion that this subcortical structure plays a central role in the coordination and/or transition between different activity states (Arcaro et al., 2018; Bourgeois et al., 2020). Accordingly, recent studies combining pulvinar inactivation with electrophysiological recordings in cortical cortex indicate that the pulvinar is a core element in gating contextual interactions between regions (Purushothaman et al., 2012; Zhou et al., 2016; de Souza et al., 2020; see also Jaramillo et al., 2019 for a computational model).

### 4.3. Contribution to different behavioral domains

To characterize the role of the five pulvinar clusters identified by connectivity analysis, we identified their co-activation patterns during task-based fMRI, and then meta-analytically decoded them. A similar meta-analysis of pulvinar activations was recently performed with another database (i.e. BrainMap, Barron et al., 2015) and reported that the pulvinar is mainly involved in the cognition domain, and to a lesser degree in action, emotion, and perception. However, this study could not identify specific functional roles associated with individual clusters. This was made possible in the current work because our clustering analysis (based on functional rest connectivity) was independent from functional decoding (based on co-activation patterns), unlike in Barron et al. (2015) where both clustering and decoding were based on co-activation patterns.

Previous work suggested that the inferior and ventrolateral parts of the pulvinar are primarily associated with striate and extra-striate cortices and thus involved in visual processes (Benevento and Rezak, 1976; Adams et al., 2000), whereas the dorsolateral and medial parts are coupled with 'higher' cortices and involved in either associative or limbic functions (Yeterian and Pandya, 1985; Romanski et al., 1997; Gutierrez et al., 2000). Our results converge with this view by demonstrating that our lateral and inferior clusters are linked to visual areas in both functional connectivity and co-activation analyses. However, these clusters were also coupled with higher-level areas in dorsolateral prefrontal and parietal cortex, suggesting a more integrative role than previously proposed. In particular, the lateral cluster was differentially associated with action (Wilke et al., 2018) and positively correlated with topics related to cognition, suggesting a role in selective attention and planning (Grieve et al., 2000; Bridge et al., 2016). On the other hand, the inferior cluster was associated with perception of faces and objects, as well as memory (see also, Yuan et al., 2017). Such division between lateral and inferior clusters is reminiscent of a segregation between dorsal and ventral visual streams, respectively (Goodale and Milner, 1992).

In contrast, the anterior pulvinar seems consistently implicated in sensorimotor functions (Jones, 2012; Kaas, 2012). Indeed, the anterior cluster exhibited strong connectivity with primary sensorimotor areas and correlated with the action domain. Moreover, its correlation with networks implicated in cognition including language and task-related performance suggests this sub-region may subserve motor selection and programming functions (Krauzlis et al., 2013; Mizzi and Michael, 2014) rather than elementary motor action itself (Acuña et al., 1983).

Finally, both the ventromedial and dorsomedial clusters were associated with emotion domain in agreement with previous findings on medial pulvinar (Ward et al., 2007; Arend et al., 2015). However, network coupled to the dorsomedial cluster encompassed key nodes of the salience network (Seeley et al., 2007; Menon and Uddin, 2010) and thus correlated with pain and motor topics, suggesting a role in the control of attention and detection of behaviorally relevant stimuli. This may accord with impaired filtering of salient distractors in patients with damage to the dorsal part of the pulvinar (Lucas et al., 2019). On the other hand, the ventromedial cluster was coupled with widely distributed areas but showed predominant task-based co-activation patterns in medial temporal lobe and limbic structures such as the hippocampus and amygdala, loading on topics related to the recognition of faces and emotional faces as well as memory. This dovetails with previous findings that ventromedial pulvinar could play a role in allocating affective values to incoming sensory stimuli (Padmala et al., 2010).

Collectively, our results fit with models proposing a general role of the pulvinar in attentional processes, in keeping with its widespread connections with multiple sensory systems and higher-level cerebral areas associated with top-down attention control (Saalmann et al., 2012; Fiebelkorn and Kastner, 2019a; Bourgeois et al., 2020). According to this view, it could be speculated that the different sub-regions of the pulvinar make different contributions to these processes, by coordinating activity within widely distributed networks. For instance, attentional selection of perceptually and emotionally salient stimuli could rely on dorsomedial and ventromedial clusters, respectively, while the lateral and inferior clusters may select information based on internal task demands and memory representations, and the anterior cluster could coordinate action selection processes. Future work manipulating specific neuronal populations within the pulvinar will be necessary to verify these conjectures.

### 4.4. Limitations

Our study provides an important step in the functional characterization of pulvinar using a data-driven approach, but several caveats should be noted. First, our parcellation is limited by the spatial resolution of fMRI. Although the HCP data provides high-quality data (Smith et al., 2013), it would be interesting to confirm our parcellation using even finer resolution (Arcaro et al., 2015). Second, our meta-analysis with Neurosynth is limited by the information available in this database (see Yarkoni et al., 2011), based on quantitative associations between frequent terms and brain coordinates in published articles, regardless of precise methodological aspects. However, random noise in the database should not bias results but rather make it more difficult to obtain significant findings, and this should be minimized by the large number of studies included. Finally, our decoding analysis was based on coarse cognitive domains, not accounting for a wider and finer evaluation of human cognition. Correlations observed with particular topics are meaningful only in relative terms. The low correlation scores in this analysis might be explained by the fact that all brain voxels are considered in the analysis even those with a null value (e.g., the map related to the 'motor' topic may have no voxel activated in the visual cortex). Conversely, however, high correlation scores might reflect a strong co-activation specificity. In any case, a statistical comparison of correlation scores would not be trivial in this case given 1) the high number of

degrees of freedom associated with the large number of voxels tested, and 2) it is extremely unlikely that two models of brain activity associated with different domains can be completely disconnected, and therefore using a test to reject the null value cannot be applied. For these reasons, our approach provides a qualitative descriptive comparison only. Nevertheless, considered across the different domains and different clusters, these data allow highlighting both the functional heterogeneity and the major putative roles of pulvinar subregions in a comprehensive and objective manner.

## 5. Conclusion

In sum, our data provide new insight into the functional organization and role of the human pulvinar. By combining data-driven analysis of resting-state connectivity and meta-analysis, we were able to identify five distinct functional clusters with particular co-activation patterns and links with specific behavioral domains. These results provide novel evidence of a key role of the pulvinar in coordinating information processing and communication across distributed brain networks.

## Declaration of competing interest

None.

## CRediT authorship contribution statement

**Carole Guedj:** Conceptualization, Data curation, Formal analysis, Investigation, Methodology, Project administration, Resources, Software, Validation, Visualization, Writing - original draft, Writing - review & editing. **Patrik Vuilleumier:** Conceptualization, Funding acquisition, Methodology, Project administration, Supervision, Validation, Writing - review & editing.

## Acknowledgments

This work was supported by a project grant from the Swiss National Science Foundation to PV [grant number 320030_166704]. Data were provided by the Human Connectome Project, WU-Minn Consortium (Principal Investigators: David Van Essen and Kamil Ugurbil; 1U54MH091657) funded by the 16 NIH Institutes and Centers that support the NIH Blueprint for Neuroscience Research; and by the McDonnell Center for Systems Neuroscience at Washington University.

## Appendix A. Supplementary data

Supplementary data to this article can be found online at https://doi.org/10.1016/j.neuroimage.2020.117162.

## References

Acuña, C., Gonzalez, F., Dominguez, R., 1983. Sensorimotor unit activity related to intention in the Pulvinar of behaving Cebus Apella monkeys. Exp. Brain Res. 52, 411–422.
Adams, M.M., Hof, P.R., Gattass, R., Webster, M.J., Ungerleider, L.G., 2000. Visual cortical projections and chemoarchitecture of macaque monkey pulvinar. J. Comp. Neurol. 419, 377–393.
Arcaro, M.J., Pinsk, M.A., Chen, J., Kastner, S., 2018. Organizing principles of pulvino-cortical functional coupling in humans. Nat. Commun. 9, 5382.
Arcaro, M.J., Pinsk, M.A., Kastner, S., 2015. The anatomical and functional organization of the human visual pulvinar. J. Neurosci. 35, 9848–9871.
Arend, I., Henik, A., Okon-Singer, H., 2015. Dissociating emotion and attention functions in the pulvinar nucleus of the thalamus. Neuropsychology 29, 191.
Arend, I., Rafal, R., Ward, R., 2008. Spatial and temporal deficits are regionally dissociable in patients with pulvinar lesions. Brain 131, 2140–2152.
Baizer, J.S., Desimone, R., Ungerleider, L.G., 1993. Comparison of subcortical connections of inferior temporal and posterior parietal cortex in monkeys. Vis. Neurosci. 10, 59–72.
Baleydier, C., Morel, A., 1992. Segregated thalamocortical pathways to inferior parietal and inferotemporal cortex in macaque monkey. Vis. Neurosci. 8, 391–405.
Barron, D.S., Eickhoff, S.B., Clos, M., Fox, P.T., 2015. Human pulvinar functional organization and connectivity. Hum. Brain Mapp. 36, 2417–2431.
Bender, D.B., 1981. Retinotopic organization of macaque pulvinar. J. Neurophysiol. 46, 672–693.
Benevento, L.A., Rezak, M., 1976. The cortical projections of the inferior pulvinar and adjacent lateral pulvinar in the rhesus monkey (Macaca mulatta): an autoradiographic study. Brain Res. 108, 1–24.
Berman, R.A., Wurtz, R.H., 2011. Signals conveyed in the pulvinar pathway from superior colliculus to cortical area MT. J. Neurosci. 31, 373–384.
Berridge, C.W., Waterhouse, B.D., 2003. The locus coeruleus–noradrenergic system: modulation of behavioral state and state-dependent cognitive processes. Brain Res. Rev. 42, 33–84.
Bertini, C., Pietrelli, M., Braghittoni, D., Làdavas, E., 2018. Pulvinar lesions disrupt fear-related implicit visual processing in hemianopic patients. Front. Psychol. 9. Available at: https://www.frontiersin.org/articles/10.3389/fpsyg.2018.02329/full. (Accessed 14 November 2019). Accessed.
Blei, D.M., Ng, A.Y., Jordan, M.I., 2003. Latent dirichlet allocation. J. Mach. Learn. Res. 3, 993–1022.
Bourgeois, A., Guedj, C., Carrera, E., Vuilleumier, P., 2020. Pulvino-cortical interaction: an integrative role in the control of attention. Neurosci. Biobehav. Rev. Available at: http://www.sciencedirect.com/science/article/pii/S0149763418307991. (Accessed 23 January 2020) Accessed.
Bridge, H., Leopold, D.A., Bourne, J.A., 2016. Adaptive pulvinar circuitry supports visual cognition. Trends Cognit. Sci. 20, 146–157.
Cauda, F., Cavanna, A.E., D'agata, F., Sacco, K., Duca, S., Geminiani, G.C., 2011. Functional connectivity and coactivation of the nucleus accumbens: a combined functional connectivity and structure-based meta-analysis. J. Cognit. Neurosci. 23, 2864–2877.
Corbetta, M., Patel, G., Shulman, G.L., 2008. The reorienting system of the human brain: from environment to theory of mind. Neuron 58, 306–324.
Corbetta, M., Shulman, G.L., 2002. Control of goal-directed and stimulus-driven attention in the brain. Nat. Rev. Neurosci. 3, 201–215.
Cotton, P.L., Smith, A.T., 2007. Contralateral visual hemifield representations in the human pulvinar nucleus. J. Neurophysiol. 98, 1600–1609.
Cox, R.W., 1996. AFNI: software for analysis and visualization of functional magnetic resonance neuroimages. Comput. Biomed. Res. 29, 162–173.
de Souza, B.O.F., Cortes, N., Casanova, C., 2020. Pulvinar modulates contrast responses in the visual cortex as a function of cortical hierarchy. Cerebr. Cortex 30, 1068–1086.
DeSimone, K., Viviano, J.D., Schneider, K.A., 2015. Population receptive field estimation reveals new retinotopic maps in human subcortex. J. Neurosci. 35, 9836–9847.
Fiebelkorn, I.C., Kastner, S., 2019a. Functional specialization in the attention network. Annu. Rev. Psychol.
Fiebelkorn, I.C., Kastner, S., 2019b. The puzzling pulvinar. Neuron 101, 201–203.
Fiebelkorn, I.C., Pinsk, M.A., Kastner, S., 2019. The mediodorsal pulvinar coordinates the macaque fronto-parietal network during rhythmic spatial attention. Nat. Commun. 10, 215.
Fox, M.D., Snyder, A.Z., Vincent, J.L., Corbetta, M., Essen, D.C.V., Raichle, M.E., 2005. The human brain is intrinsically organized into dynamic, anticorrelated functional networks. PNAS 102, 9673–9678.
Gattass, R., Oswaldo-Cruz, E., Sousa, A.P., 1978. Visuotopic organization of the cebus pulvinar: a double representation the contralateral hemifield. Brain Res. 152, 1–16.
Gattass, R., Soares, J.G.M., Lima, B., 2018. The role of the pulvinar in spatial visual attention. In: Gattass, R., Soares, J.G.M., Lima, B. (Eds.), The Pulvinar Thalamic Nucleus of Non-human Primates: Architectonic and Functional Subdivisions, 57–60 Advances in Anatomy, Embryology and Cell Biology. Springer International Publishing, Cham. https://doi.org/10.1007/978-3-319-70046-5_12. Available at: (Accessed 11 November 2019). Accessed.
Glasser, M.F., Sotiropoulos, S.N., Wilson, J.A., Coalson, T.S., Fischl, B., Andersson, J.L., Xu, J., Jbabdi, S., Webster, M., Polimeni, J.R., Van Essen, D.C., Jenkinson, M., 2013. The minimal preprocessing pipelines for the Human Connectome Project. Neuroimage 80, 105–124.
Goodale, M.A., Milner, A.D., 1992. Separate visual pathways for perception and action. Trends Neurosci. 15, 20–25.
Grieve, K.L., Acuña, C., Cudeiro, J., 2000. The primate pulvinar nuclei: vision and action. Trends Neurosci. 23, 35–39.
Guedj, C., Meunier, D., Meunier, M., Hadj-Bouziane, F., 2017. Could LC-NE-dependent adjustment of neural gain drive functional brain network reorganization? Neural Plast. 2017:4328015.
Gutierrez, C., Cola, M.G., Seltzer, B., Cusick, C., 2000. Neurochemical and connectional organization of the dorsal pulvinar complex in monkeys. J. Comp. Neurol. 419, 61–86.
Gutierrez, C., Yaun, A., Cusick, C.G., 1995. Neurochemical subdivisions of the inferior pulvinar in macaque monkeys. J. Comp. Neurol. 363, 545–562.
Handl, J., Knowles, J., Kell, D.B., 2005. Computational cluster validation in post-genomic data analysis. Bioinformatics 21, 3201–3212.
Hutchison, R.M., Everling, S., 2012. Monkey in the middle: why non-human primates are needed to bridge the gap in resting-state investigations. Front. Neuroanat. 6. Available at: https://www.frontiersin.org/articles/10.3389/fnana.2012.00029/full. (Accessed 22 November 2019). Accessed.
Hwang, K., Bertolero, M.A., Liu, W.B., D'Esposito, M., 2017. The human thalamus is an integrative hub for functional brain networks. J. Neurosci. 37, 5594–5607.
Jain, A.K., Murty, M.N., Flynn, P.J., 1999. Data Clustering: A Review.
Janssen, R.J., Jylänki, P., Kessels, R.P.C., van Gerven, M.a.J., 2015. Probabilistic model-based functional parcellation reveals a robust, fine-grained subdivision of the striatum. Neuroimage 119, 398–405.
Jaramillo, J., Mejias, J.F., Wang, X.-J., 2019. Engagement of pulvino-cortical feedforward and feedback pathways in cognitive computations. Neuron 101, 321–336 e9.

Jeub, L.G.S., Sporns, O., Fortunato, S., 2018. Multiresolution consensus clustering in networks. Sci. Rep. 8, 1–16.
Jo, H.J., Saad, Z.S., Simmons, W.K., Milbury, L.A., Cox, R.W., 2010. Mapping sources of correlation in resting state FMRI, with artifact detection and removal. Neuroimage 52, 571–582.
Jones, E.G., 2001. The thalamic matrix and thalamocortical synchrony. Trends Neurosci. 24, 595–601.
Jones, E.G., 2012. The Thalamus. Springer Science & Business Media.
Kaas, J.H., 2012. Somatosensory system. In: The Human Nervous System. Elsevier, pp. 1074–1109. Available at: https://linkinghub.elsevier.com/retrieve/pii/B9780123742360100306. (Accessed 21 November 2019). Accessed.
Kaas, J.H., Lyon, D.C., 2007. Pulvinar contributions to the dorsal and ventral streams of visual processing in primates. Brain Res. Rev. 55, 285–296.
Kahnt, T., Chang, L.J., Park, S.Q., Heinzle, J., Haynes, J.-D., 2012. Connectivity-based parcellation of the human orbitofrontal cortex. J. Neurosci. 32, 6240–6250.
Kanai, R., Komura, Y., Shipp, S., Friston, K., 2015. Cerebral hierarchies: predictive processing, precision and the pulvinar. Philos. Trans. R. Soc. Lond. B Biol. Sci. 370.
Kastner, S., O'Connor, D.H., Fukui, M.M., Fehd, H.M., Herwig, U., Pinsk, M.A., 2004. Functional imaging of the human lateral geniculate nucleus and pulvinar. J. Neurophysiol. 91, 438–448.
Krauth, A., Blanc, R., Poveda, A., Jeanmonod, D., Morel, A., Székely, G., 2010. A mean three-dimensional atlas of the human thalamus: generation from multiple histological data. Neuroimage 49, 2053–2062.
Krauzlis, R.J., Lovejoy, L.P., Zénon, A., 2013. Superior colliculus and visual spatial attention. Annu. Rev. Neurosci. 36, 165–182.
Leh, S.E., Chakravarty, M.M., Ptito, A., 2008. The connectivity of the human pulvinar: a diffusion tensor imaging tractography study. Int. J. Biomed. Imag. 1–5, 2008.
Lucas, N., Bourgeois, A., Carrera, E., Landis, T., Vuilleumier, P., 2019. Impaired visual search with paradoxically increased facilitation by emotional features after unilateral pulvinar damage. Cortex 120, 223–239.
Márquez-Legorreta, E., Horta-Júnior, J. de AC., Berrebi, A.S., Saldaña, E., 2016. Organization of the zone of transition between the pretectum and the thalamus, with emphasis on the pretectothalamic lamina. Front. Neuroanat. 10, 82.
McCallum, A.K., 2002. MALLET: a machine learning for language. Available at: http://mallet.cs.umass.edu.
Meilă, M., 2007. Comparing clusterings—an information based distance. J. Multivariate Anal. 98, 873–895.
Menon, V., Uddin, L.Q., 2010. Saliency, switching, attention and control: a network model of insula function. Brain Struct. Funct. 214, 655–667.
Mizzi, R., Michael, G.A., 2014. The role of the collicular pathway in the salience-based progression of visual attention. Behav. Brain Res. 270, 330–338.
Monti, S., Tamayo, P., Mesirov, J., Golub, T., 2003. Consensus clustering: a resampling-based method for class discovery and visualization of gene expression microarray data. Mach. Learn. 52, 91–118.
Morel, A., Magnin, M., Jeanmonod, D., 1997. Multiarchitectonic and stereotactic atlas of the human thalamus. J. Comp. Neurol. 387, 588–630.
Morris, J.S., Ohman, A., Dolan, R.J., 1999. A subcortical pathway to the right amygdala mediating "unseen" fear. Proc. Natl. Acad. Sci. U.S.A. 96, 1680–1685.
Mueller, S., Wang, D., Fox, M.D., Yeo, B.T.T., Sepulcre, J., Sabuncu, M.R., Shafee, R., Lu, J., Liu, H., 2013. Individual variability in functional connectivity architecture of the human brain. Neuron 77, 586–595.
Müller, E., Munn, B., Hearne, L.J., Smith, J.B., Fulcher, B., Cocchi, L., Shine, J.M., 2020. Core and matrix thalamic sub-populations relate to spatio-temporal cortical connectivity gradients. Neuroscience. Available at: http://biorxiv.org/lookup/doi/10.1101/2020.02.28.970350. (Accessed 23 May 2020). Accessed.
Murphy, K., Birn, R.M., Bandettini, P.A., 2013. Resting-state fMRI confounds and cleanup. Neuroimage 80, 349–359.
Neau, J.P., Bogousslavsky, J., 1996. The syndrome of posterior choroidal artery territory infarction. Ann. Neurol. 39, 779–788.
Nichols, T., Brett, M., Andersson, J., Wager, T., Poline, J.-B., 2005. Valid conjunction inference with the minimum statistic. Neuroimage 25, 653–660.
Olszewski, J., 1952. The Thalamus of the Macaca Mulatta: an Atlas for Use with the Stereotaxic Instrument. Karger.
Op de Beeck, H.P., 2010. Against hyperacuity in brain reading: spatial smoothing does not hurt multivariate fMRI analyses? Neuroimage 49, 1943–1948.
Padmala, S., Lim, S.-L., Pessoa, L., 2010. Pulvinar and affective significance: responses track moment-to-moment stimulus visibility. Front. Hum. Neurosci. 4.
Petersen, S.E., Robinson, D.L., Morris, J.D., 1987. Contributions of the pulvinar to visual spatial attention. Neuropsychologia 25, 97–105.
Poldrack, R.A., 2011. Inferring mental states from neuroimaging data: from reverse inference to large-scale decoding. Neuron 72, 692–697.
Poldrack, R.A., Mumford, J.A., Schonberg, T., Kalar, D., Barman, B., Yarkoni, T., 2012. Discovering relations between mind, brain, and mental disorders using topic mapping. PLoS Comput. Biol. 8, e1002707.
Power, J.D., Barnes, K.A., Snyder, A.Z., Schlaggar, B.L., Petersen, S.E., 2012. Spurious but systematic correlations in functional connectivity MRI networks arise from subject motion. Neuroimage 59, 2142–2154.
Purushothaman, G., Marion, R., Li, K., Casagrande, V.A., 2012. Gating and control of primary visual cortex by pulvinar. Nat. Neurosci. 15, 905–912.
Quax, S., Jensen, O., Tiesinga, P., 2017. Top-down control of cortical gamma-band communication via pulvinar induced phase shifts in the alpha rhythm. PLoS Comput. Biol. 13, e1005519.
Romanski, L.M., Giguere, M., Bates, J.F., Goldman-Rakic, P.S., 1997. Topographic organization of medial pulvinar connections with the prefrontal cortex in the rhesus monkey. J. Comp. Neurol. 379, 313–332.
Rousseeuw, P.J., 1987. Silhouettes: a graphical aid to the interpretation and validation of cluster analysis. J. Comput. Appl. Math. 20, 53–65.
Saalmann, Y.B., 2014. Intralaminar and medial thalamic influence on cortical synchrony, information transmission and cognition. Front. Syst. Neurosci. 8, 83.
Saalmann, Y.B., Pinsk, M.A., Wang, L., Li, X., Kastner, S., 2012. The pulvinar regulates information transmission between cortical areas based on attention demands. Science 337, 753–756.
Schneider, K.A., 2011. Subcortical mechanisms of feature-based attention. J. Neurosci. 31, 8643–8653.
Seeley, W.W., Menon, V., Schatzberg, A.F., Keller, J., Glover, G.H., Kenna, H., Reiss, A.L., Greicius, M.D., 2007. Dissociable intrinsic connectivity networks for salience processing and executive control. J. Neurosci. 27, 2349–2356.
Sherman, S.M., 2016. Thalamus plays a central role in ongoing cortical functioning. Nat. Neurosci. 19, 533–541.
Sherman, S.M., Guillery, R.W., 2002. The role of the thalamus in the flow of information to the cortex. Philos. Trans. R. Soc. Lond. B Biol. Sci. 357, 1695–1708.
Shipp, S., 2001. Corticopulvinar connections of areas V5, V4, and V3 in the macaque monkey: a dual model of retinal and cortical topographies. J. Comp. Neurol. 439, 469–490.
Shipp, S., 2003. The functional logic of cortico-pulvinar connections. Philos. Trans. R. Soc. Lond. B Biol. Sci. 358, 1605–1624.
Shipp, S., 2004. The brain circuitry of attention. Trends Cognit. Sci. 8, 223–230.
Smith, S.M., et al., 2013. Resting-state fMRI in the human connectome project. Neuroimage 80, 144–168.
Smith, S.M., Fox, P.T., Miller, K.L., Glahn, D.C., Fox, P.M., Mackay, C.E., Filippini, N., Watkins, K.E., Toro, R., Laird, A.R., Beckmann, C.F., 2009. Correspondence of the brain's functional architecture during activation and rest. PNAS 106, 13040–13045.
Stepniewska, I., Kaas, J.H., 1997. Architectonic subdivisions of the inferior pulvinar in new world and old world monkeys. Vis. Neurosci. 14, 1043–1060.
Stitt, I., Zhou, Z.C., Radtke-Schuller, S., Fröhlich, F., 2018. Arousal dependent modulation of thalamo-cortical functional interaction. Nat. Commun. 9, 2455.
Tian, Y., Margulies, D.S., Breakspear, M., Zalesky, A., 2020. Topographic organization of the human subcortex unveiled with functional connectivity gradients. Neuroscience. Available at: http://biorxiv.org/lookup/doi/10.1101/2020.01.13.903542. (Accessed 10 June 2020). Accessed.
Toro, R., Fox, P.T., Paus, T., 2008. Functional coactivation map of the human brain. Cerebr. Cortex 18, 2553–2559.
Van Dijk, K.R.A., Sabuncu, M.R., Buckner, R.L., 2012. The influence of head motion on intrinsic functional connectivity MRI. Neuroimage 59, 431–438.
Van Essen, D.C., Smith, S.M., Barch, D.M., Behrens, T.E.J., Yacoub, E., Ugurbil, K., Wu-Minn HCP Consortium, 2013. The Wu-minn human connectome project: an overview. Neuroimage 80, 62–79.
Wager, T.D., Lindquist, M.A., Nichols, T.E., Kober, H., Van Snellenberg, J.X., 2009. Evaluating the consistency and specificity of neuroimaging data using meta-analysis. Neuroimage 45, S210–S221.
Ward, R., Calder, A.J., Parker, M., Arend, I., 2007. Emotion recognition following human pulvinar damage. Neuropsychologia 45, 1973–1978.
Ward, R., Danziger, S., Owen, V., Rafal, R., 2002. Deficits in spatial coding and feature binding following damage to spatiotopic maps in the human pulvinar. Nat. Neurosci. 5, 99–100.
Wilke, M., Schneider, L., Dominguez-Vargas, A.-U., Schmidt-Samoa, C., Miloserdov, K., Nazzal, A., Dechent, P., Cabral-Calderin, Y., Scherberger, H., Kagan, I., Bähr, M., 2018. Reach and grasp deficits following damage to the dorsal pulvinar. Cortex 99, 135–149.
Yarkoni, T., Poldrack, R.A., Nichols, T.E., Essen, D.C.V., Wager, T.D., 2011. Large-scale automated synthesis of human functional neuroimaging data. Nat. Methods 8, 665–670.
Yeterian, E.H., Pandya, D.N., 1985. Corticothalamic connections of the posterior parietal cortex in the rhesus monkey. J. Comp. Neurol. 237, 408–426.
Yuan, R., Taylor, P.A., Alvarez, T.L., Misra, D., Biswal, B.B., 2017. MAPBOT: meta-analytic parcellation based on text, and its application to the human thalamus. Neuroimage 157, 716–732.
Zhou, H., Schafer, R.J., Desimone, R., 2016. Pulvinar-cortex interactions in vision and attention. Neuron 89, 209–220.